Planta (2007) 226:989–1005
DOI 10.1007/s00425-007-0545-8

ORIGINAL ARTICLE

The citrus fruit proteome: insights into citrus fruit metabolism

E. Katz · M. Fon · Y. J. Lee · B. S. Phinney · A. Sadka · E. Blumwald

Received: 3 April 2007 / Accepted: 5 May 2007 / Published online: 31 May 2007
© Springer-Verlag 2007

Abstract Fruit development and ripening are key processes in the production of the phytonutrients that are essential for a balanced diet and for disease prevention. The pathways involved in these processes are unique to plants and vary between species. Climacteric fruit ripening, especially in tomato, has been extensively studied; yet, ripening of non-climacteric fruit is poorly understood. Although the different species share common pathways; developmental programs, physiological, anatomical, biochemical composition and structural differences must contribute to the operation of unique pathways, genes and proteins. Citrus has a non-climacteric fruit ripening behavior and has a unique anatomical fruit structure. For the last few years a citrus genome-wide ESTs project has been initiated and consists of 222,911 clones corresponding to 19,854 contigs and 37,138 singletons. Taking advantage of the citrus database we analyzed the citrus proteome. Using LC-MS/MS we analyzed soluble and enriched membrane fractions of mature citrus fruit to identify the proteome of fruit juice cells. We have identified ca. 1,400 proteins from these fractions by searching NCBI-nr (green plants) and citrus ESTs databases, classified these proteins according to their putative function and assigned function according to known biosynthetic pathways.

Keywords Citrus sinensis · Juice sac cell · LC-MS/MS · Sugar metabolism · Vesicle trafficking · Citrate metabolism

Electronic supplementary material The online version of this article (doi:10.1007/s00425-007-0545-8) contains supplementary material, which is available to authorized users.

E. Katz · M. Fon · E. Blumwald (✉)
Department of Plant Sciences, University of California,
Davis, CA 95616, USA
e-mail: eblumwald@ucdavis.edu

Y. J. Lee · B. S. Phinney
Genome Center, University of California, Davis, CA 95616, USA

A. Sadka
Department of Fruit Tree Species, ARO,
The Volcani Center, 50250 Bet Dagan, Israel

Introduction

Fruit development and ripening are key processes in the production of the phytonutrients that are essential for a balanced diet and for disease prevention. The pathways involved in these processes are unique to plants and vary between species. Climacteric fruit ripening, especially in tomato, has been extensively studied; yet, ripening of non-climacteric fruit is poorly understood.

Citrus is the most important evergreen fruit crop in world trade and has a non-climacteric fruit ripening behavior and a unique anatomical fruit structure. Morphologically, the citrus fruit is composed of two major sections, the pericarp, and the endocarp, which is the edible part of the fruit (Spiegel-Roy and Goldschmidt 1996). The pericarp itself is composed of two distinct portions, the epicarp, known also as the 'flavedo' and the internal portion, the mesocarp, known as the albedo both are defined as the 'peel.' During the early stages of fruit development the albedo, the internal part of the mesocarp, occupy 60–90% of fruit volume. When the pulp grows, the albedo become gradually thinner and in some cases such as mandarins it is degraded and disappears leaving only the vascular bundles between the peel and pulp segments. The pulp segments filled with juice sacs are initiated during flowering and gradually develop (Spiegel-Roy and Goldschmidt 1996). Juice sacs accumulate sugars and organic acid and therefore are the ultimate sink part of the fruit. Fruit sugar content change during development and determine to a great extent the TSS (total soluble solids) of the fruit. The TSS, together with the total fruit acidity are key fruit quality determinants and determine whether the fruit can be marketed. Total sugar content in the fruit is determined by the relative influence of three processes: sugar transport, sugar metabolism, and storage. Most of the cell sugars and organic acids are being stored in the vacuoles, which occupy up to 95% of the juice sac cell volume. The understanding of the mechanisms regulating sugars and acids metabolism, transport, and storage is vital to the development of practices that would warrant optimal sugar concentrations and acidity in the fruit at harvest and the development of post-harvest practices to enhance fruit quality.

Proteomics is becoming a powerful tool in plant research in the last few years. The development of state-of-the-art LC-MS/MS technology, fine separation techniques, development of genomic, and ESTs databases for a variety of species and powerful bio-informatics tools enable the understanding and assessment of protein function, their relative abundance, the modifications affecting enzyme activity, their interaction with other proteins and localization. Proteomics research has been conducted in several plant species mainly using 2DE gels. Most successful studies are those which use separation of subcellular compartments such as mitochondria (Bardel et al. 2002; Heazlewood et al. 2004; Kruft et al. 2001; Lister et al. 2004; Millar et al. 2001), chloroplast (Friso et al. 2004; Giacomelli et al. 2006; Kleffmann et al. 2004; Koch 2004; Lonosky et al. 2004; Peltier et al. 2000), endoplasmic reticulum (Maltman et al. 2002), peroxisomes (Fukao et al. 2002), cell walls (Slabas et al. 2004), plastoglobules (Ytterberg et al. 2006), and vacuoles (Carter et al. 2004) since they contain a limited number of proteins which help in protein identification.

The large scale sequencing and analysis of the citrus ESTs database is a fundamental part of genomics research to enable gene discovery and annotation. For the last few years a citrus genome-wide ESTs project has been initiated and already consists of 157,608 clones corresponding to 19,854 contigs and 37,138 singletons (http://cgf.ucdavis.edu). Here, we describe the first attempt to analyze citrus fruit proteome using LC-MS/MS and the citrus genome-wide ESTs database, focusing on mature juice cells, and aiming at the identification of pathways acting in the last phase of citrus fruit development, affecting fruit quality determined by pre- and post-harvest processes.

Materials and methods

Plant material

Mature Navel orange (Citrus sinensis cv Washington) fruits at stage III of development (Katz et al. 2004), 200 days after flowering, were obtained from the Lindcove Research and Extension Center, University of California. Juice sac tissues were collected and used immediately. Soluble and membrane-enriched fractions from juice sacs were prepared as described elsewhere (Müller et al. 1997) with slight modifications. The juice sacs were ground in homogenization buffer containing 0.5 M MOPS–KOH pH 8.5, 1.5% PVPP, 7.5 mM EDTA, 2 mM DTT, 0.1 mM PMSF, and 0.1% (v/v) of protease inhibitor cocktail (Sigma, St. Louis, MO, USA). The homogenates were filtered through four layers of cheesecloth and centrifuged at 1,500*g* for 20 min to eliminate cellular debris and nuclei. The pellet was discarded and the supernatant was centrifuged at 12,000*g* for 20 min at 4°C. The pellet containing the mitochondria-enriched fraction was immediately frozen until further use. The supernatant was then subjected to ultracentrifugation at 100,000*g* for 60 min at 4°C. The supernatant, containing soluble proteins was treated as described below. The microsomal pellet obtained was resuspended in a buffer containing 10 mM Tris–Mes pH 7.6, 10% (w/w) glycerol, 20 mM KCl, 1 mM EDTA, 2 mM DTT, 0.1 mM PMSF, and 0.1% (v/v) of protease inhibitor cocktail (Sigma) and layered onto a 20, 34, and 40% sucrose step gradient (Blumwald and Poole 1987). After centrifugation at 80,000*g* for 2.5 h at 4°C, the 0%/20% interface containing tonoplast-enriched membranes, the 20%/34% interface containing ER/Golgi-enriched membranes and the 34%/40% interface containing plasma membrane (PM)-enriched fractions were recovered. The membranes were diluted with buffer containing 5 mM Tris–MES pH 7.6, 10% glycerol, and 0.1% (w/w) of protease inhibitor cocktail (Sigma), sedimented at 100,000*g* and resuspended in 0.4–1.0 ml of the same buffer.

Digestion and pre-fractionation of each subcellular fractions

Soluble fraction

Soluble proteins were precipitated in ammonium sulfate (85%) and collected by centrifugation at 12,000 × *g*. The pellets were resuspended in a buffer containing 10 mM KH_2PO_4 and 0.5 mM DTT and de-salted with PD-10 columns (Amersham Bioscience, GE Healthcare, Piscataway, NJ, USA) according to manufacturer's instructions. The resulting elute was then concentrated using Amicon YM-3 Centricon concentrators (Millipore, Bedford, MA, USA) at 3,000 × *g*. The samples were concentrated to a final volume of about 1 ml. Protein concentration was determined using the detergent-compatible protein assay (Bio-Rad, Hercules, CA, USA) and stored in 50% glycerol at −180°C. The soluble proteins (SOL) were digested in-solution with an urea digestion protocol. Briefly, 1 mg of soluble proteins were dissolved in 8 M urea-200 mM Tris buffer (pH 7.8), reduced with dithiothreitol, alkylated by iodoacetamide, diluted to 2 M urea, and treated with trypsin (Modified trypsin, sequencing grade: Promega, Madison, WI, USA) at 1:50 enzyme to substrate ratio (w/w) overnight at 37°C.

Membrane fractions

Plasma membrane, tonoplast, and ER/Golgi fraction (ER/Go) were digested with a triple digestion protocol. Briefly, 1 mg of each fraction was dissolved in 2 M CNBr in acetonitrile and formic acid at 1:4 ratio (v/v), incubated overnight at room temperature in the dark, and then lyophilized. The dry proteins were washed twice with water in order to completely remove CNBr and formic acid, and were re-dissolved in 8 M urea-200 mM Tris buffer (pH 7.8), reduced with dithiothreitol, alkylated by iodoacetamide, diluted with 4 M urea, and digested with Lys-C (sequencing grade, Sigma) at 1:50 enzyme to substrate ratio (w/w) overnight at 37°C. Lys-C was de-activated by boiling for 5 min. Each sample was diluted with 2 M urea and digested with trypsin overnight at 37°C.

Mitochondria Fraction

Because of difficulties in removing non-protein contaminations from the mitochondrial fraction (MIT), the proteins were first separated in one-dimensional 10% SDS-PAGE gel, the proteins were in-gel digested, and analyzed by mass spectrometry. Briefly, 100 μg of MIT was resolved on SDS-PAGE gel and stained with colloidal Coomassie blue. The gel was cut into 1 mm^3 pieces and transferred to microcentrifuge tubes. Dehydration of the gel pieces was done by 100 mM ambic [ammonium bicarbonate, Fluka Chemie GmbH, Steinheim, Germany) for 5 min and then, the buffer discarded. The gel pieces were treated with 50 μl 100% acetonitrile for 15 min at room temperature and dried completely in a speadvac. The gel pieces were rehydrated by the addition of 50 μl of 10 mM DTT in 100 mM ambic, and reduction was performed at 56°C for 30 min. The DTT solution was decanted, and 100% acetonitrile was added followed by incubation at room temperature for 3–5 min (twice) and drying using a speedvac for 15 min. Alkylation was done by the addition of 50 μl of 55 mM iodoacetamide in 100 mM ambic for 20 min in the dark at room temperature. After discarding the supernatant, the proteins were washed briefly with 100 mM ambic and replaced with fresh 100 mM ambic for another wash for 15 min at room temperature. Afterwards, the liquid was decanted, 50 μl 100% acetonitrile were added and the mixture was incubated for 15 min at room temperature, followed by drying. The gel pieces were rehydrated with a 50 mM ambic buffer containing 13 ng/μl trypsin (sequencing grade modified, Promega). The gel pieces were incubated over night at 37°C, and liquid was collected after centrifugation at 13,000×*g* for 3 min. Peptide extraction was performed by adding 15–30 μl of 60% acetonitrile/1%TFA to each of gel pieces, sonication for 10 min and centrifugation for 30 s. Supernatants were collected and added to the supernatants collected before, the solution dried, 8 μl of 3% TFA in water were added, and the samples were sonicated for 5 min. Samples were desalted, concentrated and purified by ZipTip pipette tips containing C18 reverse phase (RP) media (Millipore Corporation) according to the manufacturer instructions.

Separation of digested peptides by strong cation exchange chromatography (SCX)

In-solution digested peptides were further fractionated by strong cation exchange chromatography (SCX) prior to on-line RP LC-MS/MS analysis. Trypsin digested samples were dried and redissolved in ~200 μl of Solvent A (see below Mobile phase A) and then injected onto a polysulfoethyl A cation exchange column (100 × 2.1 mm^2, 5 μm diameter, and 300 Å pore size) from PolyLC, Columbia, MD, USA with a flow rate of 200 μl/min utilizing the mobile phases as described elsewhere (http://www.proteomecenter.org/): mobile phase A contained 5 mM potassium phosphate (pH 3.0) and 25% acetonitrile; mobile phase B contained 5 mM potassium phosphate (pH 3.0), 25% acetonitrile and 350 mM potassium chloride. After each sample was loaded, the run was isocratic for 15 min at 100% mobile phase A, and peptides were eluted using a linear gradient of 0–25% B over 30 min followed by a linear gradient of 25–100% B in 20 min and then held for 5 min at 100% B. Fractions at 2 min intervals were collected and concentrated by vacuum centrifugation.

LC-MS/MS analysis

SCX fractionated membrane samples

The SCX fractions were loaded sequentially on an home-made on-line trap column (0.25 × 30 mm^2, Magic C18AQ, 5 μm, and 100 Å) at a flow rate of 10 μl/min with buffer A (see below). After application and removal of salt and urea, the flow rate was decreased to 300 nl/min, and the trap column effluent was switched to a home-made fritless RP microcapillary column (0.1 × 180 mm^2; packed with Magic C18AQ, Michrom Bio Resources, Auburn, CA, USA, 5 μm, and 100 Å) as described elsewhere (Gatlin et al. 1998). The RP separation of peptides was performed using a Paradigm MG4, Michrom Bio Resources with buffers of 5% acetonitrile-0.1% formic acid (buffer A) and 80% acetonitrile-0.1% formic acid (buffer B) using a 150 min gradient (0–10% B for 20 min, 10–45% for

110 min, and 45–100% B for 20 min). Peptide analysis was performed utilizing a LCQ Deca XP Plus (Thermo, San Jose, CA, USA) coupled directly to an LC column. An MS survey scan was obtained for the m/z range of 400–1,400, and MS/MS spectra were acquired for the three most intense ions from the survey scan. An isolation mass window of 3.0 Da was used for the pre-cursor ion selection and normalized collision energy of 35% was used for the fragmentation. Dynamic exclusion for 2 min duration was used to acquire MS/MS spectra from low intensity ions.

In-gel digested mitochondria fraction

Each digested MIT gel band was run over on-line LC-MS/MS without SCX fractionation. Finnigan LTQ-FT, a hybrid ion trap Fourier transform mass spectrometer (Thermo), connected with Finnigan Micro-AS autosampler and Surveyor MS LC pump (Thermo) was used for this analysis. Trap column ($0.15 \times 20\ mm^2$; Magic C18AQ, 3 μm, and 100 Å) and analytical column ($0.07 \times 180\ mm^2$; Magic C18AQ, 3 μm, and 100 Å) were home-made and used. Other LC conditions, both trap and analytical column, buffers, and loading and analytical flow rates, etc., are essentially the same with those for the Michrom LC system described above.

An MS survey scan was obtained with Fourier Transform mass spectrometer for the m/z range of 300–1,600 with resolution setting at 100,000 and MS/MS spectra were acquired with LTQ ion trap for the ten most intense ions from the survey scan. An isolation mass window of 2.0 Da was used for the pre-cursor ion selection and normalized collision energy of 35% was used for the fragmentation. Dynamic exclusion for 1 min duration and rejection of acquisition of singly charged ion were used.

Data analysis

Database searching

Tandem mass spectra were extracted by Bioworks 3.2 (Thermo-Electron, San Jose CA, USA) and converted to Mascot generic format (MGF). Charge state de-convolution and de-isotoping were not performed. All MS/MS samples were analyzed using X!Tandem (www.thegpm.org) Version 2006.09.15.3 and Mascot (http://www.matrixscience.com) Version 2.1.03 and searched against the Citrus EST database acquired from the University of California at Davis genomics facility (http://cgf.ucdavis.edu) and the University of California at Riverside (HarvEST Citrus, http://harvest.ucr.edu), and a database of common laboratory artifacts and all currently available green plant sequences in the NCBI non-redundant database. The Following X!Tandem search options were turned on when performing the search; search for point mutations, search for partial cleavage's and search against reverse database sequences.

Criteria for protein identification

Scaffold (Version Scaffold-01_06_03, Proteome Software Inc., Portland, OR, USA) was used to validate MS/MS based peptide and protein identifications. Peptide identifications were accepted if they could be established at >95.0% probability as specified by the Peptide Prophet algorithm (Keller et al. 2002). Protein identifications were accepted if they could be established at >99.0% probability and contained at least two identified peptides. Protein probabilities were assigned by the Protein Prophet algorithm (Nesvizhskii et al. 2003). Proteins that contained similar peptides and could not be differentiated based on MS/MS analysis alone were grouped to satisfy the principles of parsimony.

Results and discussion

Protein identification by searching databases using LC-MS/MS data and functional classification

LC-MS/MS analysis of the citrus juice sacs proteins resulted in the detection of 1,394 unique proteins. The peptide sequences were identified by searching the databases with uninterpreted fragment ion mass spectra using MASCOT (Perkins et al. 1999). The search was conducted against the NCBI non-redundant protein (green plants) database and the Citrus ESTs database (http://cgf.ucdavis.edu). From the 1,394 proteins identified, 433 were ER/Golgi-associated, 502 were PM-associated, 329 were associated with the tonoplast, 657 were mitochondria-associated, and 479 were soluble proteins (Table 1). It should be noted that our experimental design precluded the differentiation between cytosolic and other soluble proteins located in the different cell compartments' milleau. The complete list of identified proteins is shown in Supplemental Table 1. The identified proteins were sorted into functional categories (Fig. 1; Table 1) using TAIR (http://www.arabidopsis.org/), GO (http://www.geneontology.org/), UniProt (http://www.pir.uniprot.org/), Pfam (http://pfam.janelia.org/), InterPro (http://www.ebi.ac.uk/interpro/), and NCBI (http://www.ncbi.nlm.nih.gov/). The assignment of putative roles into known eukaryotic biosynthetic pathways was performed using KEGG (http://www.genome.jp/kegg/) and TAIR (AraCyc) (http://www.arabidopsis.org/biocyc/index.jsp). We assigned function to 1,247 proteins, while 146 proteins remained unclassified. To simplify the discussion in this paper, proteins were classified into 12 major functional groups (Fig. 1; Table 1). The most abundant class of citrus

Table 1 Classification of proteins identified after searching the citrus ESTs and NCBI-nr databases by Mascot and X!Tandem using LC-MS/MS uninterpreted spectra according to their abundance in the isolated fractions

Citrus ESTs and NCBI-nr databases	ER/Golgi		Plasma membrane		Soluble		Tonoplast		Mitochondria		Total	
	Number	%	Number	%	Number	%	Number	%	Number	%	Number	%
Chaperone/HSP	45	10.4	51	10.2	65	13.6	34	10.3	40	6.1	235	9.8
Energy	21	4.8	27	5.4	5	1.0	13	4.0	60	9.1	126	5.3
Metabolism	59	13.6	84	16.7	195	40.7	39	11.9	132	20.1	509	21.2
Oxidative process	27	6.2	28	5.6	46	9.6	18	5.5	32	4.9	151	6.3
Processing	33	7.6	37	7.4	53	11.1	25	7.6	35	5.3	183	7.6
Signaling	39	9.0	38	7.6	31	6.5	20	6.1	35	5.3	163	6.8
Structure	17	3.9	21	4.2	8	1.7	9	2.7	13	2.0	68	2.8
Trafficking	42	9.7	44	8.8	11	2.3	36	10.9	61	9.3	194	8.1
Transcription	2	0.5	2	0.4	2	0.4	0	0	3	0.5	9	0.4
Translation	62	14.3	85	16.9	34	7.1	60	18.2	58	8.8	299	12.5
Transport	52	12.0	59	11.8	1	0.2	59	17.9	82	12.5	253	10.5
Unknown	34	7.9	26	5.2	28	5.8	16	4.9	106	16.1	210	8.8
Total	433	100	502	100	479	100	329	100	657	100	2,400	100

Proteins were classified into 12 major groups and are represented according to fractions analyzed. Note, that most protein were found in more than one fraction, therefore, the total number of proteins represented in the table is higher than the total amount of proteins identified (see also Fig. 1)

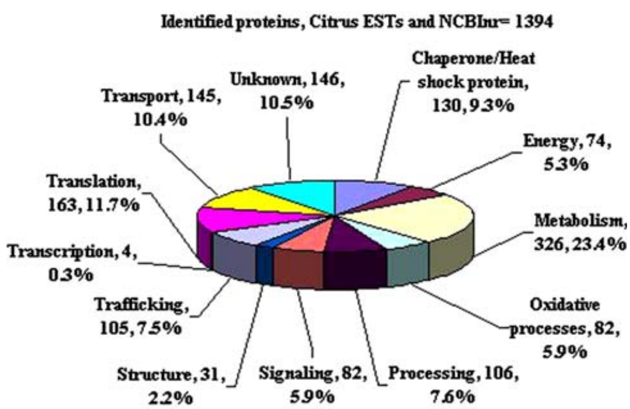

Fig. 1 Functional classification analysis of LC-MS/MS identified proteins. The number and percentage of proteins from each functional class from the total combined number of proteins from citrus fruit juice sacs are shown. Total proteins identified after Mascot and X!Tandem searching against the Citrus ESTs database and NCBI-non-redundant protein database

juice sac proteins were those involved in metabolic processes (23.4%) followed by translation (11.7%) and transport (10.4%). A considerable high number of proteins was classified as chaperons/heat shock (9.3%), processing (7.6%), trafficking (7.5%), and signaling (5.9%). Proteins involved in other main cellular activities were also detected, such as oxidative processes (5.9%), energy (5.3%), and structure (2.2%). Proteins with no predicted function were classified as unknown (10.5%).

Because of the predominant roles that acids and sugars play in determining fruit quality, we are focusing our discussion on proteins and pathways that are associated with citrate metabolism, and sugar synthesis and degradation.

Citric acid cycle

Citric acid is the main organic acid found in citrus fruit juice cells (Shimada et al. 2006; Vandercook 1977). Most of the enzymes acting in the citric acid cycle were identified in our study including pyruvate dehydrogenase (E1, E2, and E3 subunits), citrate synthase, aconitate hydratase, NADP+ isocitrate dehydrogenase (IDH), 2-oxoglutarate dehydrogenase complex (subunits E1, E2, and E3), succinyl-CoA ligase, succinate dehydrogenase, fumarate hydratase, and malate dehydrogenase (MDH) (Fig. 2; Table 2). Citrate can be produced by either the condensation of oxaloacetate and acetyl-CoA catalyzed by citrate synthase (EC 2.3.3.1) or by ADP + phosphate + acetyl-CoA + oxaloacetate catalyzed by ATP-citrate synthase (or ATP:citrate lyase and ACL; EC 2.3.3.8), both enzymes were found juice cell sacs (Fig. 2; Table 2). Three citrate synthase were identified, CTG1107592 and CTG11111984, homologous to At3g58750 (*CSY2*), and At2g42790 (*CSY3*), respectively, both are localized to the Arabidopsis peroxisome (Pracharoenwattana et al. 2005) and CTG1105142 homologous to the mitochondrial At2g44350 (*CYS4*). One ACL, homologous to the cytosolic At3g06650 was also identified in the soluble fraction. The next step in the citrate cycle is the conversion of citrate to isocitrate by aconitase (EC 4.2.1.3). We identified three aconitase isozymes; CTG1104713 and CTG1104288 (homologous to At4g35830 and At2g05710,

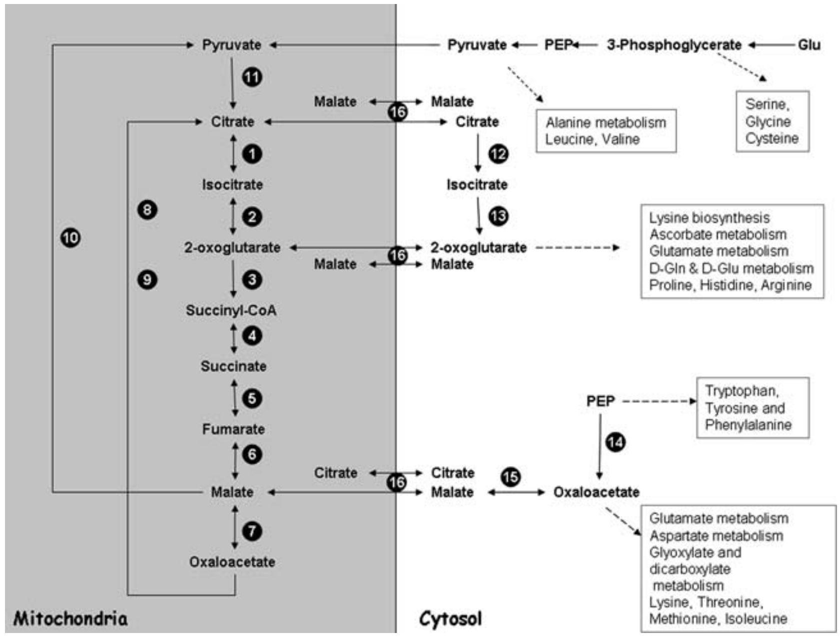

Fig. 2 Enzymes acting in the citric acid cycle identified after searching the citrus ESTs and NCBI-nr databases by Mascot and X!Tandem using LC-MS/MS uninterpreted spectra according to their abundance in the isolated citrus juice cells fractions. (1) *Aconitase*, (2) *Isocitrate dehydrogenase*, (3) *2-oxoglutarate dehydrogenase complex*: *E1-Oxoglutarate dehydrogenase*, *E2-dihydrolipoamide*, *E3-Dihydrolipoyl dehydrogenase*, (4) *Succinyl CoA synthetase*, (5) *Succinate dehydrogenase*, (6) *Fumarase*, (7) *Malate dehydrogenase*, (8) *Citrate synthase*, (9) ATP citrate lyase, (10) *Malic enzyme*, (11) *Pyruvate dehydrogenase*, (12) Cytosolic aconitase, (13) Cytosolic isocitrate dehydrogenase, (14) PEP carboxylase, (15) Cytosolic malate dehydrogenase, and (16) Dicarboxylate/tricarboxylate carrier (CTG1104002). Amino acids metabolism pathways identified in our search and branched out the citric acid cycle are shown

respectively) and one homologous to At2g05710 found in the mitochondria fraction (Table 2). From our experiments, we cannot conclude whether the citrus soluble aconitase isozymes are located in the mitochondria matrix or in the cytosol, since the soluble fraction includes proteins from both compartments. The oxidative decarboxylation of isocitrate into 2-oxoglutarate is mediated by the action of IDH (EC 1.1.1.42). Three IDH citrus accessions were identified; two mitochondrial NAD^+-dependent, CTG1093369 and CTG1107030, homologous to At4g35260, and At5g03290, respectively, and a $NADP^+$-dependent, CTG1102843, homologous to At1g65930. In addition, three more isoforms that were not found in the citrus EST database were identified by a NCBI-nr search; two cytosolic $NADP^+$-dependent, homologous to At5g14590 and At1g54340, and a mitochondrial NAD^+-dependent (homologous to At4g35650). The presence of NAD^+- (and $NADP^+$-) dependent mitochondrial and cytosolic IDH support the notion that citrate might be transported from the mitochondria and metabolized to (via cytosolic aconitase) isocitrate and 2-oxoglutarate in the cytosol of the citrus juice sac cells. The 2-oxoglutarate dehydrogenase complex catalyzes the overall conversion of 2-oxoglutarate to succinyl-CoA and CO_2. It contains multiple copies of three enzymatic components: 2-oxoglutarate dehydrogenase (E1; EC 1.2.4.2), dihydrolipoamide succinyltransferase (E2; EC 2.3.1.61) and lipoamide dehydrogenase (E3; EC 1.8.1.4). All three enzymes were identified in the juice cells. Two isoforms of 2-oxoglutarate dehydrogenase (E1) were identified; CTG1106938 (homologous to the Arabidopsis At3g55410) and another isoform, homologous to At5g65750, was identified by a NCBI-nr database search. Dihydrolipoamide succinyltransferase (E2), CTG1100133 (homologous to the Arabidopsis At5g55070), was identified in the mitochondria and catalyzes the conversion of S-succinyldihydrolipoyl to succinyl-CoA. Two lipoamide dehydrogenase proteins (E3), CTG1104273 (homologous to the Arabidopsis At3g17240) and an isoform, homologous to At1g48030, were identified in the mitochondria and the PM fractions. These proteins mediate the conversion of S-succinyldihydrolipoyl to lipoamide, which in turn is catalyzed to S-succinyldihydrolipoyl by 2-oxoglutarate dehydrogenase. Succinyl-CoA is then converted succinate by succinyl-CoA ligase (EC 6.2.1.4). Three citrus contigs were found in our search, CTG1096641 (homologous of the Arabidopsis At5g08300) and CTG1108914 and CTG1100890, homologous to At2g20420, which were all found in the mitochondria fraction. In addition, one isoform (homologous to the Arabidopsis At5g23250) not present in the citrus database was found in the PM fraction. Succinate is oxidized to fumarate by the succinate dehydrogenase complex with the simultaneous conversion of a FAD co-factor into FADH2 (EC

Table 2 Enzymes acting in the citric acid cycle identified after searching the citrus ESTs and NCBI-nr databases by Mascot and X!Tandem using LC-MS/MS uninterpreted spectra according to their abundance in the isolated citrus juice cells fractions

Enzyme description	Citrus contig	GI numbers of homologous found in NCBI-nr	Arabidopsis homologous	Fraction
Citrate synthase	CTG1107592	gi|28716243, gi|46209065, gi|56528008, gi|56528009	At3g58750	M
	CTG1111984	gi|46209066, gi|61690401	At2g42790	M
	CTG1105142	gi|37509375, gi|42477097, gi|45452868, gi|45453349[a]	At2g44350	M
		gi|40646744, gi|1352088	At2g44350	M
		gi|50251779	At2g42790	M
ATP:citrate lyase		gi|15919087	At3g06650	S
Aconitase	CTG1104713	gi|28390556, gi|28618139, gi|28618921, gi|28618922[a]	At4g35830	S
	CTG1104288	gi|34519552, gi|38037656, gi|38037658, gi|42477701[a]	At2g05710	S, P
		gi|2145473, gi|29027432	At2g05710	M
NAD+ dependent isocitrate dehydrogenase	CTG1093369	gi|38031036, gi|38031038, gi|38031188, gi|38031190	At4g35260	M
	CTG1107030	gi|34519262, gi|34522209, gi|34522303, gi|46213765[a]	At5g03290	M, P
		gi|46805298, gi|15237075, gi|50910073, gi|7431336	At4g35650	M
NADP+ dependent isocitrate dehydrogenase	CTG1102843	gi|21652333, gi|29180472, gi|34524312, gi|38039192[a]	At1g65930	S, M, E, T
		gi|7573308, gi|3021512, gi|7431243, gi|3021513, gi|7431245	At5g14590	S, E
		gi|15221788, gi|2623962, gi|19171610, gi|25283701	At1g54340	E
2-oxoglutarate dehydrogenase complex	CTG1106938	gi|42477897, gi|46211819, gi|46211820, gi|46215960[a]	At3g55410	M, P, E
2-oxoglutarate dehydrogenase (E1)		gi|2827711	At5g65750	P
Dihydrolipoamide succinyltransferase (E2)	CTG1100133	gi|57873898, gi|57873899, gi|57879348	At5g55070	M
Lipoamide dehydrogenase (E3)	CTG1104273	gi|29550326, gi|34418495, gi|34523702, gi|34523798[a]	At3g17240	M, P, S
		gi|23321340	At1g48030	M, P
Succinyl-CoA ligase	CTG1096641	gi|63059521, gi|63065640	At5g08300	M
	CTG1100890	gi|57871816, gi|57871817	At2g20420	M
	CTG1108914	gi|38033768, gi|46209439, gi|46209929	At2g20420	M
		gi|34393512, gi|50938629	At5g23250	P
Succinate dehydrogenase	CTG1107716	gi|46214927, gi|55399520, gi|56534741, gi|57933946	At5g66760	M, E, P
	CTG1104192	gi|28617666, gi|28617667, gi|34419014, gi|46209278[a]	At2g18450	M
	CTG1099546	gi|55291046, gi|55291047, gi|57569607, gi|57573536	At3g27380	M
Fumarate hydratase	CTG1105176	gi|28617886, gi|28617887, gi|34519470, gi|37509403[a]	At2g47510	M
Malate dehydrogenase	CTG1098368	gi|31671825, gi|31672450, gi|57569742, gi|57569743[a]	At3g15020	E
	CTG1105400	gi|21650749, gi|34418755, gi|34519844, gi|46208709[a]	At3g15020	M
	CTG1098208	gi|34432137, gi|34432507, gi|57873152, gi|57873153[a]	At3g47520	M
	CTG1103261	gi|21650796, gi|28615865, gi|34418936, gi|34519953[a]	At5g43330	T
	CTG1098006	gi|31671200, gi|31671346, gi|31671967, gi|31672244[a]	At5g43330	M

Table 2 continued

Enzyme description	Citrus contig	GI numbers of homologous found in NCBI-nr	Arabidopsis homologous	Fraction
		gi|1524121, gi|2286153, gi|2827082, gi|18202485, gi|7431164[a]	At1g04410	S
		gi|7431179, gi|2827078	At2g22780	M
		gi|50834461, gi|6469139, gi|60593476, gi|60593494, gi|126894	At5g09660	M
Malic enzyme	CTG1095849	gi|63055838, gi|63056722, gi|63056817, gi|63058812[a]	At2g19900	T, P, S
		gi|1346485, gi|228412, gi|20469	At1g79750	S
	CTG1109050	gi|21650831, gi|34518997, gi|57932149	At4g00570	M, P
Pyruvate dehydrogenase	CTG1095175	gi|62428557, gi|62429025, gi|68138986	At1g59900	S, E, P
Complex	CTG1104320	gi|28618511, gi|28716051, gi|34519451, gi|34520138[a]	At1g59900	M
Pyruvate dehydrogenase (E1)	CTG1104330	gi|21650840, gi|28617942, gi|28617943, gi|29550868[a]	At5g50850	M
		gi|1709454	At5g50850	M
		gi|50948007	At5g50850	M
Dihydrolipoamide acetyltransferase (E2)		gi|11994364, gi|18400212, gi|20260138	At3g13930	M
Dihydrolipoamide dehydrogenase (E3)	CTG1104273	gi|29550326, gi|34418495, gi|34523702, gi|34523798[a]	At3g17240	P, M, S
		gi|14916975	At1g48030	P
		gi|23321340	At1g48030	M

M mitochondria, *S* soluble, *P* plasma membrane, *T* tonoplast, *E* ER/Golgi

[a] For many of the peptide mass spectra there were additional matching accessions in the databases. For the full list of matching proteins see supplemental Table 1

1.3.5.1). We identified three proteins assigned as citrus ESTs CTG1107716, CTG1104192, and CTG1099546, which are homologous to the Arabidopsis mitochondrial succinate dehydrogenase At5g66760, At2g18450, and At3g27380, respectively. We also identified fumarate hydratase, a mitochondrial protein encoded by CTG1105176 (homologous to the Arabidopsis At2g47510) that mediates the interconversion of fumarate to malate. The last step of the pathway, the interconversion of malate to oxaloacetate utilizing NAD^+/NADH is catalyzed by MDH (EC 1.1.1.37). In eukaryotic cells, MDH is usually found in the mitochondrial matrix and in the cytosol. We identified five citrus contigs CTG1098368 (soluble) and CTG1105400 (mitochondrial), both homologous to At3g15020, CTG1098208 (homologous to the mitochondrial At3g47520), and CTG1103261 (soluble) and CTG1098006 (mitochondrial) (both homologous to At5g43330). Three additional MDH isoforms homologous to At1g04410 (cytosolic), At2g22780 and At5g09660 (both mitochondrial) were identified by NCBI-nr search. Most of these proteins were found mainly in the mitochondria-enriched fraction and in the soluble fraction.

In addition to the conversion of malate to oxaloacetate, mediated by MDH, malate can also be converted to pyruvate by malic enzyme (ME). Two types of ME are known, NAD-dependent (EC 1.1.1.39) catalyzing the reaction: malate + NAD^+ = pyruvate + CO_2 + NADH, and NADP-dependent (EC 1.1.1.40): malate + $NADP^+$ = pyruvate + CO_2 +NADPH) (Wheeler et al. 2005). In plants, NAD-dependent isoforms function predominantly in the mitochondria while the NADP-dependent isoforms are found in the cytosol and plastids. We identified few MEs, CTG1095849 (At2g19900 homologous) and an homologous to At1g79750 found in the soluble fraction, both are NADP-dependent type, and known as AtNADP-ME1 and AtNADP-ME4, respectively (Wheeler et al. 2005). CTG1109050 (homologous to At4g00570), an NAD-dependent type, was also found in the mitochondria fraction. ME enables plants mitochondria to metabolize PEP derived from glycolysis via an alternative pathway. Malate can be synthesized from PEP in the cytosol via PEP carboxylase and MDH (Fig. 2). These suggest that some of the MDHs that were identified in our study (see above) are cytosolic and act in this pathway. In addition, four PEP-carboxylase were identified, two in the citrus database search, CTG1095231 (homologous to At4g37870) and CTG1105152 (homologous to At2g42600) and two, homologous to At3g14940 and At1g53310 were identified in the NCBI-nr database search (Supplemental Table 1). In addition, we identified a dicarboxylate/tricarboxylate carrier or mitochondrial 2-oxoglutarate/malate carrier protein, CTG1104002 (homologous to At5g19760), which might be responsible for transporting malate, 2-oxoglutarate and citrate across the mitochondria inner membrane (Fig. 2).

Citric acid, which accounts for most of the titratable acidity in citrus fruit cells, is reduced during citrus fruit development (Shimada et al. 2006). Our data suggest that during the acid decline stage, citrate may be utilized by three major metabolic pathways for sugar production, amino acid synthesis and acytyl-CoA metabolism. Sadka et al. (2000a, b) suggested that citrate is accumulated in the vacuole and during fruit development is released to the cytosol and metabolized into isocitrate by cytosolic aconitase and then into 2-oxoglutarate by NADP-IDH. 2-oxoglutarate can be then metabolized to amino acid production such as glutamate as found for tomato fruits (Boggio et al. 2000; Gallardo et al. 1995). Aspartate and alanine aminotransferases and glutamate dehydrogenase have been reported to be involved in glutamate synthesis (Boggio et al. 2000; Bortolotti et al. 2003). The increase in aspartate and alanine aminotransferase transcripts was detected during citrus fruit development by microarrays analysis (Cercos et al. 2006). Bortolotti et al. (2003) suggested that glutamate production is being balanced by utilization into glutamine and catabolism through the γ-aminobutyric acid (GABA) shunt. Indeed, we have identified enzymes that mediate the conversion of citrate into glutamate metabolism and GABA shunt to succinate-semialdehyde and succinate (Fig. 3; Supplemental Table 1), providing further support to the notion of the conversion of citrate into amino acids during the stage III of citrus fruit development. Aconitase, NADP-IDH, glutamine synthetase, glutamate decarboxylase, GABA aminotransferase, and succinate semialdehyde dehydrogenase were identified in our proteomic analysis confirming the microarray data recently published showing increased expression of all these genes (Cercos et al. 2006). In addition, many of the enzymes, including ATP-citrate lyase (ACL; homologous to At3g06650) 'initiating' the acetyl-CoA metabolism pathway have been identified in our proteomic analysis (Fig. 3; Supplemental Table 1). Cercos et al. (2006) showed a decrease in ACL expression during fruit development and ruled out the importance of acetyl-CoA metabolism in citrate catabolism pathway. However, in our experiments we could identify ACL in the mature juice cells and other enzymes acting in acetyl-CoA metabolism such as HMG-CoA synthase and HMG-CoA reductase in the mevalonate pathway and chalcone synthase and chalcone isomerase in the narigenin pathway (Fig. 3; Supplemental Table 1). Therefore, the role of acetyle-CoA metabolism in citrus fruit acid decline needs further examination. In tomato fruit, glutamate accumulates during fruit development and it has been suggested that free amino acid accumulation is part of the fruit ripening process (Boggio et al. 2000; Gallardo et al. 1995). In citrus fruit juice cells, glutamate levels are high only at stage I of fruit development (data not shown), then decrease to low and constant level during

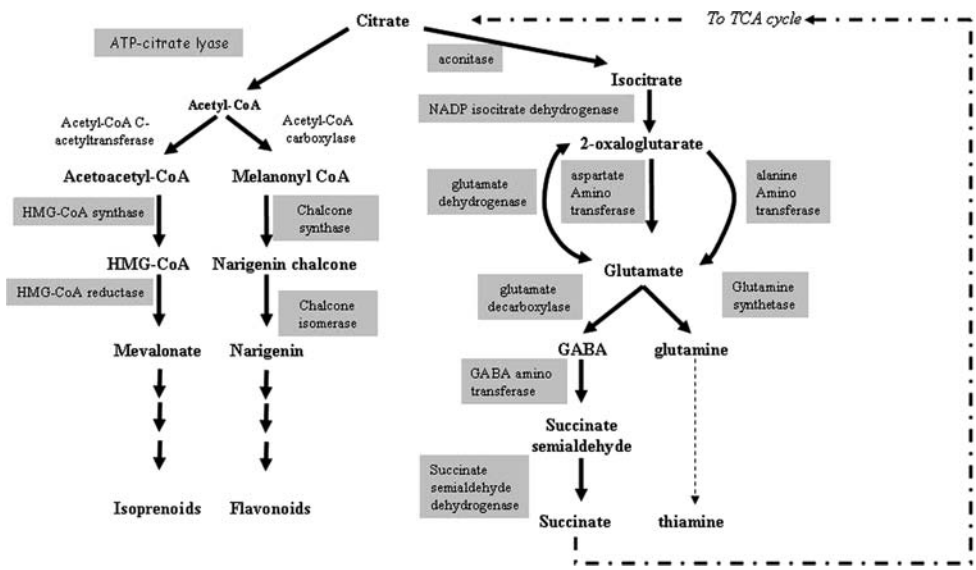

Fig. 3 Enzymes acting in citric acid metabolism identified after searching the citrus ESTs and NCBI-nr databases by Mascot and X!Tandem using LC-MS/MS uninterpreted spectra according to their abundance in the isolated citrus juice cells fractions. Enzymes marked in *gray* were found in our search, representing two possible pathways for citric acid metabolism in the mature citrus fruit

stages II and III (Cercos et al. 2006). Thus, glutamate utilization during fruit development is an important step in the homeostatic control of glutamate in the mature fruit. Two pathways for glutamate utilization were suggested: conversion of glutamate to glutamine and GABA shunt catabolism pathway (Cercos et al. 2006). Our proteomic data support this hypothesis revealing the expression of glutamine synthase acting in the glutamine synthesis pathway and glutamate decarboxylase, GABA amino transferase and succinate semialdehyde dehydrogenase in the GABA shunt pathway (Fig. 3; Supplemental Table 1).

Sugar synthesis transport and metabolism

In addition to acid content, sugar content and sugar metabolism are major contributors to fruit quality. Sugars are translocated by the phloem from source to sink tissues and uploaded into cells either symplasticaly or apoplasticaly by plasmodesmata or the action of sugar transporters, respectively (Lalonde et al. 2004). Phloem unloading is a key process in sugars partitioning because to a large extent it determines the movement of assimilates from the sieve elements to the recipient sink cells (Patrick 1997). It has been shown that unloading routes may differ according to sink type, sink development stage, sink function, growth conditions, and alternative unloading pathways may even exist in sinks with symplastically interconnecting phloem (Oparka and Turgeon 1999; Patrick 1997; Roberts et al. 1997; Viola et al. 2001). Other studies showed that plasmodesmatal conductivity can be programmatically reduced (Baluska et al. 2001; Itaya et al. 2002) and that sugar transporters can operate in parallel to predominant symplastic phloem pathways (Kuhn et al. 2003). In tomato fruits, phloem unloading pathway is symplastic during early stages, and apoplastic during later fruit developmental stages (Ruan and Patrick 1995). In some tissues, such as developing seeds and grains, and fleshy fruits, when plasmadesmatal connections between cells are absent or limited, the PM can be exposed to abundant sucrose and/or hexoses (Koch 1996). Among the fleshy fruits species that accumulate high concentrations of soluble sugars, only grape, apple, and citrus have been studied. An apoplastic mode of phloem unloading was shown for all three species (Koch and Avigne 1990; Patrick 1997; Zhang et al. 2004). Citrus fruit juice sacs are not connected simplastically to the vascular system, which provides water and assimilates to the fruit. Juice sacs obtain their supply over long distances of post-phloem, through non-vascular cell-to-cell apoplastic transport (Koch and Avigne 1990; Lowell et al. 1989). Sucrose is the major sugar translocated in the plant, and the major photoasymilate stored in the plant. Sucrose can be transported into the cells by sucrose transporters or can be degraded by cell wall invertases to glucose and fructose, which in turn can be carried by hexose transporters (Koch 2004). Few members of the sugar transporters family were identified (Table 3); CTG1108654, an hexose transporter, CTG1105250 and CTG1106455, probable glucose transporters, CTG1107685, putative sucrose transporter, and glucose-6-phosphate antiporter (Table 3). Sucrose transported into the juice cell can be metabolized in three ways; degraded by sucrose synthase or by cytosolic invertase in the cytosol or transported into the vacuole for storage. Sucrose synthase (EC 2.4.1.13) catalyzes the degradation of sucrose into UDP-glucose and fructose. Few sucrose synthases have been identified in our study (Table 3); CTG1104251, CTG1098335, and CTG1097731 (homologous to At*SUS1*) and an homologous to At*SUS2*. Three sucrose synthases were already been identified in citrus fruits (Komatsu et al. 2002), however only one of them, CTG1104251 (also known as *CitSUSA*), was identified in

Table 3 Enzymes acting in sucrose homeostasis identified after searching the citrus ESTs and NCBI-nr databases by Mascot and X!Tandem using LC-MS/MS uninterpreted spectra according to their abundance in the isolated citrus juice cells fractions

<table>
<tr><th>Enzyme description</th><th>Citrus contig</th><th>GI numbers of homologous found in NCBI-nr</th><th>Arabidopsis homologous</th><th>Fraction</th></tr>
<tr><td>Sugar transporter</td><td>CTG1106455</td><td>gi|42623658, gi|55403680, gi|55933458, gi|55933460</td><td>At4g35300</td><td>T, E, P</td></tr>
<tr><td>Hexose transporter</td><td>CTG1108654</td><td>gi|56529970, gi|57932817, gi|57934229</td><td>At4g35300</td><td>T, E, P</td></tr>
<tr><td>Glucose transporter</td><td>CTG1105250</td><td>gi|29550138, gi|42623456, gi|46217371, gi|46217372[a]</td><td>At2g48020</td><td>T</td></tr>
<tr><td>Sucrose transporter</td><td>CTG1107685</td><td>gi|38327323</td><td>At1g09960</td><td>E, T, P</td></tr>
<tr><td>Glucose-6-phosphate transporter</td><td></td><td>gi|18423670, gi|20148301, gi|61608932, gi|7489258, gi|7488807[a]</td><td>At1g61800</td><td>M</td></tr>
<tr><td>Sucrose synthase</td><td>CTG1104251</td><td>gi|34521282, gi|42414503, gi|42477746, gi|42478290[a]</td><td>At4g02280</td><td>E, P, S</td></tr>
<tr><td></td><td>CTG1098335</td><td>gi|55287758, gi|55287759, gi|55291091, gi|57572085[a]</td><td>At4g02280</td><td>S</td></tr>
<tr><td></td><td>CTG1097731</td><td>gi|31669588, gi|31672535, gi|55287535, gi|55287575[a]</td><td>At5g20830</td><td>S</td></tr>
<tr><td></td><td></td><td>gi|22121990, gi|7268988, gi|6682995, gi|15235300, gi|1488570[a]</td><td>At4g02280</td><td>E, S, P</td></tr>
<tr><td></td><td></td><td>gi|6683114, gi|6682843</td><td>At3g43190</td><td>S</td></tr>
<tr><td></td><td></td><td>gi|6682995</td><td>At4g02280</td><td>S</td></tr>
<tr><td></td><td></td><td>gi|63003687, gi|16305087</td><td>At5g20830</td><td>S</td></tr>
<tr><td></td><td></td><td>gi|30349808</td><td>At5g49190</td><td>S</td></tr>
<tr><td>UTP-glucose-1-phosphate</td><td>CTG1103404</td><td>gi|28617913, gi|28617914, gi|34418639, gi|34522190[a]</td><td>At5g17310</td><td>T, E, S</td></tr>
<tr><td>Uridylyltransferase</td><td></td><td>gi|67061</td><td>At5g17310</td><td>E, S</td></tr>
<tr><td></td><td></td><td>gi|2117937</td><td>At5g17310</td><td>P</td></tr>
<tr><td></td><td></td><td>gi|28863909</td><td>At5g17310</td><td>S</td></tr>
<tr><td></td><td></td><td>gi|12585472</td><td>At5g17310</td><td>S</td></tr>
<tr><td></td><td></td><td>gi|12585489</td><td>At5g17310</td><td>S</td></tr>
<tr><td></td><td>CTG1095142</td><td>gi|62430243, gi|62430325, gi|63104454, gi|63106282</td><td>At5g17310</td><td>M</td></tr>
<tr><td>Phosphoglucomutase</td><td>CTG1093348</td><td>gi|38026260, gi|38027679, gi|38027681, gi|38030561[a]</td><td>At1g23190</td><td>E, P, S</td></tr>
<tr><td></td><td>CTG1107094</td><td>gi|34519111, gi|34521772, gi|46207460, gi|55932721[a]</td><td>At1g23190</td><td>S</td></tr>
<tr><td></td><td></td><td>gi|12643355</td><td>At1g23190</td><td>S</td></tr>
<tr><td></td><td></td><td>gi|12585330, gi|4234941</td><td>At1g23190</td><td>S</td></tr>
<tr><td></td><td></td><td>gi|21586064</td><td>At1g23190</td><td>S</td></tr>
<tr><td></td><td></td><td>gi|50918261, gi|13324798, gi|17981609, gi|12585309, gi|12585310</td><td>At1g23190</td><td>M</td></tr>
<tr><td>Sucrose-phosphate-synthase</td><td>CTG1098483</td><td>gi|1022365, gi|18375499, gi|19223854, gi|2754746</td><td>At5g20280</td><td>S</td></tr>
<tr><td>Sucrose-phosphatase</td><td>CTG1106998</td><td>gi|28190687, gi|21387099, gi|11127757, gi|11127759[a]</td><td>At2g35840</td><td>S</td></tr>
<tr><td>Hexokinase</td><td></td><td>gi|45387405, gi|18700107, gi|12644433, gi|21700789, gi|619928[a]</td><td>At4g29130</td><td>P</td></tr>
<tr><td></td><td>CTG1102350</td><td>gi|55288949, gi|55290772</td><td>At3g20040</td><td>M</td></tr>
<tr><td></td><td></td><td>gi|11066213</td><td>At4g29130</td><td>M</td></tr>
<tr><td>Fructokinase</td><td>CTG1102896</td><td>gi|14018587, gi|21650387, gi|21651247, gi|28715596[a]</td><td>At1g76550</td><td>P, S</td></tr>
<tr><td></td><td></td><td>gi|3790102</td><td>At1g76550</td><td>P</td></tr>
<tr><td></td><td>CTG1103959</td><td>gi|28618338, gi|28618339, gi|28618414, gi|34523121[a]</td><td>At3g59480</td><td>S</td></tr>
<tr><td></td><td>CTG1107531</td><td>gi|46210040, gi|46210041, gi|46215043, gi|46215044</td><td>At5g51830</td><td>S</td></tr>
<tr><td></td><td>CTG1096588</td><td>gi|63059182, gi|63059194, gi|63066933</td><td>At1g12000</td><td>S</td></tr>
<tr><td></td><td></td><td>gi|3790102</td><td>At1g76550</td><td>S</td></tr>
<tr><td></td><td></td><td>gi|45550051</td><td>At5g51830</td><td>S</td></tr>
<tr><td>Glucose-6-phosphate isomerase</td><td></td><td>gi|18056, gi|7437363, gi|18056</td><td>At5g42740</td><td>S</td></tr>
</table>

M mitochondria, *S* soluble, *P* plasma membrane, *T* tonoplast, *E* ER/Golgi

[a] For many of the peptide mass spectra there were additional matching accessions in the databases. For the full list of matching proteins see Supplemental Table 1

our study. Komatsu et al. (2002) showed that only *CitSUSA* (CTG1104251) was expressed in mature fruit. However, our data show that citrus has at least two more genes, homologous to the Arabidopsis *SUS1* and *SUS2* that are expressed in the mature fruit. Invertases, on the other hand, were not identified in mature juice sac cells, in agreement with previous data shown a decrease in invertase expression and activity during citrus fruit maturation (Echeverria and Burns 1990; Holland et al. 1999; Lowell et al. 1989; Tomlinson et al. 1991). Our findings agree with the invertase/sucrose synthase control hypothesis suggesting that invertases mediate the initiation and expansion of many new sinks and later transition to storage and maturation phase is facilitated by shifts from invertase to sucrose synthase paths of sucrose cleavage (Koch 2004).

Sucrose, in turn, is derived from hexose phosphates through the combined actions of UTP-glucose-1-phosphate uridylyltransferase (UDP-glucose pyrophosphorylase, EC 2.7.7.9), sucrose phosphate synthase (SPS) (EC 2.4.14) and sucrose phosphatase (EC 3.1.3.24) (Fig. 4; Table 3). Hexose phosphates are not only common intermediates to the pathways of synthesis and degradation of most carbohydrates, but they are also the point of convergence of these pathways. Hexose phosphates are derived either from the breakdown of sugars and polysaccharides or from triose

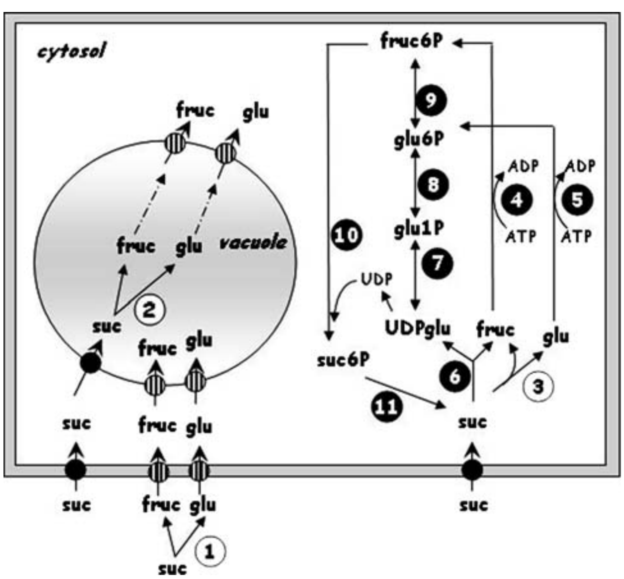

Fig. 4 Proposed model of sucrose homeostasis in citrus juice cells. Enzymes acting in sucrose homeostasis identified after searching the citrus ESTs and NCBI-nr databases by Mascot and X!Tandem using LC-MS/MS uninterpreted spectra according to their abundance in the isolated citrus juice cells fractions are marked in *black circles*. Enzymes marked in *white circles* were not found in our study. (1) Cell wall invertase, (2) acid invertase, (3) alkaline invertase (not identified), (4) fructokinase, (5) hexokinase, (6) sucrose synthase, (7) UTP-glu-1-P-Urydilyltransferase, (8) phosphoglucomutase, (9) glu-6-phosphate Isomerase, (10) suc-P-synthase, and (11) suc-phosphatase. *Suc* sucrose, *fru* fructose *glu* glucose

phosphates formed during photosynthesis and gluconeogenesis. They may be used for the synthesis of carbohydrates or for metabolism through the glycolitic and pentose phosphate pathways. The hexose phosphate pool consists of three metabolic intermediates: glucose 1-phosphate, glucose 6-phosphate, and fructose 6-phosphate. The three metabolites are kept in equilibrium through the reversible action of phosphoglucomutase and glucose-6-phosphate isomerase. Glucose phosphomutase (EC 5.4.2.2; CTG1093348 and CTG1107094; Table 3), which was also identified in our study, is an enzyme responsible for the conversion of D-glucose 1-phosphate into D-glucose 6-phosphate. Glucose phosphomutase participates in both the breakdown and synthesis of glucose and also in starch metabolism together with starch phosphorylase (EC 2.4.1.1; At3g46970), which act in starch degradation. Glucose-6-phosphate isomerase, which is involved in glycolysis and in gluconeogenesis and catalyse the conversion of D-glucose 6-phosphate to D-fructose 6-phosphate was also identified (Table 3).

Glucose and fructose can be phosphorylated to glucose-6-phosphate and fructose-6-phosphate by hexokinase (EC 2.7.1.1) and fructokinase (EC 2.7.1.4), respectively. Two hexokinase ESTs and four fructokinase were identified, all found in the soluble fraction (Table 3). UDP-glucose can be metabolized to glucose-1-phosphate by UTP-glucose-1-phosphate uridyltransferase or to sucrose-6-phosphate (with fructose-6-phosphate) by SPS. A UTP-glucose-1-phosphate uridyltransferase (EC 2.7.7.9), that mediates the reversible production of UDP-glucose and PPi from glucose-1-phosphate and UTP, was identified (Table 3). SPS, CTG1098483 (At5g20280) and sucrose phosphatase CTG1106998 (At2g35840) were also identified. Although it is well established that the cytosol is the site for sucrose synthesis via, whether sucrose is synthesized in other juice cell compartments is not yet clear. Our data would suggest that in addition to sucrose transport to the fruit there is also sucrose biosynthesis in the juice cells. All enzymes participating in the glycolysis pathway were identified; Hexokinase, glucose-6phosphate isomerase, phosphofructokinase, fructose-bisphosphate aldolase, glyceraldehyde-3-phosphate dehydrogrnase, phosphoglycerate kinase, phosphoglycerate mutase, enolase, and pyruvate kinase (Supplemental Table 1), suggesting that part of the sucrose accumulated in the fruit is used for energy production in the juice cells.

Vesicular trafficking

In plants, directed vesicle trafficking is essential for maintaining cell polarity, compartmentation, growth and development (Surpin and Raikhel 2004). Vesicle formation from a donor membrane involves the activation of small GTPases resulting in the recruitment of coat proteins (Vernoud et al. 2003) (Fig. 5). Small GTPases that have been associated in several steps in the secretory pathways comprise five distinct subfamilies; Arb, Ras, Rho, Arf, and Ran (Molendijk et al. 2004). Several Rab-like proteins (Rab2A, Rab2C, Rab6A, Rab7B, Rab7D, Rab8A, Rab8B, Rab8C, Rab11A, Rab11C, Rab11E, and Rab18), Arf-like proteins (SAR1A, SAR2, ARLA1A, and ARLA1C), Ran-like proteins (Ran1, Ran2, and Ran 3) and SEC12, associated with the different mitochondria-, ER/Golgi-, and tonoplast-enriched fractions were identified in the fruit juice sac cells and classified according to Vernoud et al. (2003). Rab proteins are localized to different intracellular compartments where they regulate vesicular trafficking. They also interact with and regulate SNAREs (see below), which are membrane proteins that provide specificity for membrane fusion events (Jurgens 2004; Sanderfoot et al. 2000; Zerial and McBride 2001). Arf proteins, comprise Arf-like and Sar proteins (Vernoud et al. 2003). Sar proteins are needed for coat protein complex II (COPII)-dependent vesicular transport from the ER to Golgi, whereas Arf-like proteins regulate COPI-dependent vesicular transport in the Golgi and clathrin-dependent budding from the trans-Golgi and the PM (Molendijk et al. 2004). SEC12, localized to the ER, is required for the recruitment of COPII coat proteins (Fig. 5; Table 4). The targeting and delivery of specific membrane and soluble proteins are carried out by a superfamily of membrane-bound

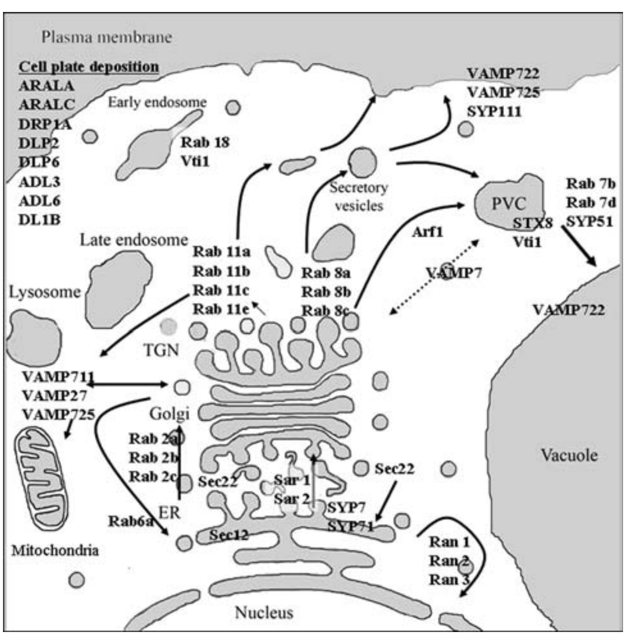

Fig. 5 Schematic representation of vesicular trafficking in citrus juice sac cells. The *diagram* indicates the vesicular trafficking-associated proteins found in our search. *Arrows* indicate traffic direction of the different intracellular vesicles. Details are provided in the text, in Table 4 and in Supplementary Table 1

and membrane-associated proteins known as SNAREs (soluble N-ethylmaleimide-sensitive factor attachment protein receptors) (Hanton et al. 2006; Pratelli et al. 2004). In general, R-SNAREs on the vesicle pairs up with 2–3 Q-SNAREs on the target membrane. In Arabidopsis, at least 54 SNAREs are divided into five subfamilies; Qa-SNAREs/syntaxins, Qb-SNARES/SNAPNs, Qc-SNAREs/SNAPCs), Qbc-SNAREs/SNAP25-like and R-SNAREs/VAMPs/synaptobrevins (Bock et al. 2001). Several members of these groups were identified (Table 4). Three syntaxins, homologous to SYP51, SYP71, and SYP111 (Tanaka et al. 2004); a Qb-SNARE (VTI12) and a Qc-SNARE (SNAP2) were identified. Among the synaptobrevins, VAMP7C, VAMP711, VAMP27, and VAMP725 were found associated with the MIT, while VAMP722 was found associated with the tonoplast and the PMs. VAMP27 and SEC22 were found associated with mitochondria/ER and mitochondria/tonoplast/ER/PM, respectively. Also, several dynamins and dynamin-like proteins were found associated with ER and PM, suggesting a putative role in clathrin-mediated vesicular trafficking. Etxeberria et al. (2005a, b, c) proposed a mechanism of sugar transport into the juice sac cells and sucrose mobilization into the juice sac cell vacuole mediated by endocytosis and intracellular vesicular trafficking. The large number of proteins associated with endocytosis and vesicular trafficking identified in our search would support this notion (Table 4; Supplemental Table 1).

Additional pathways identified by searching databases using LC-MS/MS data

We have also identified proteins participating in protein biosynthesis and degradation, transporters, H^+-ATPases (endosomal, mitochondrial, and PM-bound). In addition, major biosynthesis pathways and processes such as energy (cytochome b5, cytochrome P450, thioredoxins, glutathione reductase, NADH-ubiquinone oxireductase, etc.), signaling [calmodulin, phospholipase C2, calcium-dependent protein kinase, phosphoinositide-specific phospholipase C, phospholipase D, serine/threonine/tyrosine kinase, Remorin, annexin, 14-3-3 family proteins, polygalacturonase-inhibiting proteins, WD-40 repeat family protein/auxin-dependent protein (ARCA), etc.] oxidative processes proteins (isoflavone reductase, glutathione S-transferase, catalase, glutathione peroxidase, superoxide dismutase, ascorbate peroxidase, etc.) (Supplemental Table 1). A wide range of ribosomal proteins and heat shock proteins (HSP17, HSP26, HSP70, HSP80, HSP82, HSP90, cyclophilin-ROC7, BiP, immunophilin, etc.) were also identified. A significant number of proteins, 545 of 1,394 (39%) could not be aligned into pathways, and 146 (10.5%) proteins were classified as unknown (Fig. 1).

Table 4 Proteins acting in the vesicular trafficking pathway identified after searching the citrus ESTs and NCBI-nr databases by Mascot and X!Tandem using LC-MS/MS uninterpreted spectra according to their abundance in the isolated citrus juice cells fractions

Gene family	Protein	Citrus contig	Arabidopsis homologous	Fraction	References
Rab	Rab2A (YPT2)	CTG1103215	At4g17170	M, E, P	Sanderfoot et al. (2000), Molendijk et al. (2004), Hanton et al. (2006), Jurgens (2004), Zerial and McBride (2001), and Vernoud et al. (2003)
	Rab2C	CTG1109452	At4g35860	M	
	Rab6A		At2g44610	M	
			At2g22290	T	
	Rab7B		At3g18820	M	
	Rab7D		At1g52280	E	
	Rab8A		At3g46060	E, P	
			At5g59840	E, T, M	
	Rab8B	CTG1093502	At3g53610	M, E	
	Rab8C	CTG1105221	At5g03520	T, E	
	Rab11A		At3g46830	M	
	Rab11B	CTG1105380	At3g15060	M	
	Rab11C	CTG1106458	At1g09630	T, E, M, P	
			At1g07410	M	
	Rab11E	CTG1093843/CTG1107763	At5g45750	E	
	Rab18	CTG1106307	At1g43890	M	
Arf	SAR1A		At3g62560	T, M	Molendijk et al. (2004)
	SAR2	CTG1093323	At4g02080	M, E	
	ARLA1A	CTG1110608	At5g37680	M	
	ARLA1C	CTG1099065	At3g49870	T, E	
Ran	Ran1		At5g20010	M	Molendijk et al. (2004), Haizel et al. (1997), and Wang et al. (1997)
	Ran2		At5g20020	M, E, P	
	Ran3	CTG1096168	At5g55190	M, E, S	
	SEC12	CTG1107724	At2g01470	M	
SNAREs	Syntaxin51, SYP51	CTG1104988	At1g16240	M, T, P	Jurgens (2004), Bock et al. (2001), Uemura et al. (2004), Pratelli et al. (2004), Surpin and Raikhel (2004), and Hanton et al. (2006)
Qc-SNAREs	SYP71	CTG1110108	At3g09740	M	
	SNAP2	CTG1093336	At3g56190	M, T, E, P	
Qa-SNAREs	SYP111		At1g08350	P	
Qb-SNARE	VTI12	CTG1108789	At1g26670	M, T	
VAMP/R-SNAREs	VAMP722	CTG1104532	At2g33120	T, P	
	VAMP7C/VAMP711	CTG1108292	At4g32150	M	
	VAP27	CTG1094500/ CTG1107214	At4g21450	M	
		CTG1105906	At4g00170	M	
	VAMP725	CTG1101681	At2g32670	M	
	VAP27	CTG1097578	At2g45140	M, E	
	SEC22	CTG1107700	At1g11890	M, T, E, P	Chatre et al. (2005)
dynamin	DRP1A		At5g42080	E, P	
	DLP2	CTG1098458	At3g60190	T, E, P	
	DLP6	CTG1098626	At1g10290	E, P	
	ADL3		At1g59610	P	
	ADL6/DRP2A		At1g10290	E, P	
	DL1B		At3g61760	E	

For many of the peptide mass spectra there were additional matching accessions in the databases. For the full list of matching proteins see Supplemental Table 1

M mitochondria, *S* soluble, *P* plasma membrane, *T* tonoplast, *E* ER/Golgi

Conclusions

In this study we present a first high-throughput attempt to reveal the citrus fruit proteome. The well-developed citrus ESTs database allowed the identification of biosynthetic pathways operating in the mature fruit. The fractionation of the different soluble and membrane-bound protein fractions improved the LC-MS/MS analysis and peptide identification. In spite of the possible cross-contamination of the protein fractions, and the fact that the citrus ESTs database is still not complete and is limited to sequences isolated from specific libraries, the identification of proteins associated with different cell compartments was achieved. Our data shed light on a few processes affecting citrus fruit quality. The proteomic analysis of mature juice sac cells showed that citric acid can be utilized for the synthesis of amino acids and sugars (acid decline stage). The presence of sucrose synthase, associated with sucrose degradation, SPS and sucrose phosphatase, that mediate sucrose synthesis, suggests a role of these processes, in addition to sugar transport, in maintaining juice sac cell sugar homeostasis. Noteworthy, the presence of all of the enzymes associated with the glycolytic pathway would suggest the capacity of the juice sac cell for energy production. Interestingly, the large number of proteins associated with protein trafficking suggest an extensive vesicle transport in mature juice sac cells, providing further support to the notion of sucrose transport into citrus juice cells via an endocytic transport system (Etxeberria et al. 2005b). The proteomic analysis of the citrus fruit, initiated here, together with the future identification of the fruit metabolic pools will contribute to the further understanding of pre- and post-harvest processes and factors affecting fruit development and ripening, allowing for the development of new practices for fruit quality improvement.

Acknowledgments This work was supported by grant No. 5000-117 from the California Citrus Research Board, by a Research Grant No. US-3575-04R from BARD, the United States-Israel Binational Agricultural Research and Development Fund, and by the Will W. Lester Endowment, University of California.

References

Baluska F, Cvrckova F, Kendrick-Jones J, Volkmann D (2001) Sink plasmodesmata as gateways for phloem unloading. Myosin VIII and calreticulin as molecular determinants of sink strength? Plant Physiol 126:39–46

Bardel J, Louwagie M, Jaquinod M, Jourdain J, Luche S, Rabilloud T, Macherel D, Garin J, Bourguignon J (2002) A survey of the plant mitochondrial proteome in relation to development. Proteomics 2:880–898

Blumwald E, Poole RJ (1987) Salt tolerance in suspension cultures of sugar beet: induction of Na+/H+ antiport activity at the tonoplast by growth in salt. Plant Physiol 83:884–887

Bock JB, Matern HT, Peden AA, Scheller RH (2001) A genomic perspective on membrane compartment organization. Nature 409:839–841

Boggio SB, Palatnik JF, Heldt HW, Valle EM (2000) Changes in amino acid composition and nitrogen metabolizing enzymes in ripening fruits of *Lycopersicon esculentum* Mill. Plant Sci 159:125–133

Bortolotti S, Boggio SB, Delgado L, Orellano EG, Valle EM (2003) Different induction patterns of glutamate metabolizing enzymes in ripening fruits of the tomato mutant green flesh. Physiol Plant 119:384–391

Carter C, Pan S, Zouhar J, Avila EL, Girke T, Raikhel NV (2004) The vegetative vacuole proteome of *Arabidopsis thaliana* reveals predicted and unexpected proteins. Plant Cell 16:3285–3303

Cercos M, Soler G, Iglesias DJ, Gadea J, Forment J, Talon M (2006) Global analysis of gene expression during development and ripening of citrus fruit flesh a proposed mechanism for citric acid utilization. Plant Mol Biol 62:513–527

Chatre L, Brandizzi F, Hocquellet A, Hawes C, Moreau P (2005) Sec22 and Memb11 are v-SNAREs of the anterograde endoplasmic reticulum-golgi pathway in tobacco leaf epidermal cells. Plant Physiol 139:1244–1254

Echeverria E, Burns JK (1990) Sucrose breakdown in relation to fruit growth of acid lime (*Citrus aurantifolia*). J Exp Bot 41:705–708

Etxeberria E, Baroja-Fernandez E, Munoz FJ, Pozueta-Romero J (2005a) Sucrose-inducible endocytosis as a mechanism for nutrient uptake in heterotrophic plant cells. Plant Cell Physiol 46:474–481

Etxeberria E, Gonzalez P, Pozueta-Romero J (2005b) Sucrose transport into citrus juice cells: evidence for an endocytic transport system. J Am Soc Hortic Sci 130:269–274

Etxeberria E, Gonzalez P, Tomlinson P, Pozueta-Romero J (2005c) Existence of two parallel mechanisms for glucose uptake in heterotrophic plant cells. J Exp Bot 56:1905–1912

Friso G, Giacomelli L, Ytterberg AJ, Peltier J-B, Rudella A, Sun Q, Wijk KJv (2004) In-depth analysis of the thylakoid membrane proteome of arabidopsis thaliana chloroplasts: new proteins, new functions, and a plastid proteome database. Plant Cell 16:478–499

Fukao Y, Hayashi M, Nishimura M (2002) Proteomic analysis of leaf peroxisomal proteins in greening cotyledons of Arabidopsis thaliana. Plant Cell Physiol 43:689–696

Gallardo F, Galvez S, Gadal P, Canovas FM (1995) Changes in NADP(+)-linked isocitrate dehydrogenase during tomato fruit ripening—characterization of the predominant cytosolic enzyme from green and ripe pericarp. Planta 196:148–154

Gatlin CL, Kleemann GR, Hays LG, Link AJ, Yates JR (1998) Protein identification at the low femtomole level from silver-stained gels using a new fritless electrospray interface for liquid chromatography microspray and nanospray mass spectrometry. Anal Biochem 263:93–101

Giacomelli L, Rudella A, van Wijk KJ (2006) High light response of the thylakoid proteome in arabidopsis wild type and the ascorbate-deficient mutant *vtc2-2*. A comparative proteomics study. Plant Physiol 141:685–701

Haizel T, Merkle T, Pay A, Fejes E, Nagy F (1997) Characterization of proteins that interact with the GTPbound form of the regulatory GTPase Ran in Arabidopsis. Plant J 11:93–103

Hanton SL, Matheson LA, Brandizzi F (2006) Seeking a way out: export of proteins from the plant endoplasmic reticulum. Trends Plant Sci 11:335–343

Heazlewood JL, Tonti-Filippini JS, Gout AM, Day DA, Whelan J, Millar AH (2004) Experimental analysis of the arabidopsis mitochondrial proteome highlights signaling and regulatory components, provides assessment of targeting prediction programs, and indicates plant-specific mitochondrial proteins. Plant Cell 16:241–256

Holland N, Sala JM, Menezes HC, Lafuente MT (1999) Carbohydrate content and metabolism as related to maturity and chilling sensitivity of cv. fortune mandarins. J Agric Food Chem 47:2513–2518

Itaya A, Ma F, Qi Y, Matsuda Y, Zhu Y, Liang G, Ding B (2002) Plasmodesma-mediated selective protein traffic between symplasmically isolated cells probed by a viral movement protein. Plant Cell 14:2071–2083

Jurgens G (2004) Membrane trafficking in plants. Annu Rev Cell Dev Biol 20:481–504

Katz E, Lagunes PM, Riov J, Weiss D, Goldschmidt EE (2004) Molecular and physiological evidence suggests the existence of a system II-like pathway of ethylene production in non-climacteric Citrus fruit. Planta 219:243–252

Keller A, Nesvizhskii AI, Kolker E, Aebersold R (2002) Empirical statistical model to estimate the accuracy of peptide identifications made by MS/MS and database search. Anal Chem 74:5383–5392

Kleffmann T, Russenberger D, von Zychlinski A, Christopher W, Sjolander K, Gruissem W, Baginsky S (2004) The Arabidopsis thaliana chloroplast proteome reveals pathway abundance and novel protein functions. Curr Biol 14:354–362

Koch K (2004) Sucrose metabolism: regulatory mechanisms and pivotal roles in sugar sensing and plant development. Curr Opin Plant Biol 7:235–246

Koch KE (1996) Carbohydrate-modulated gene expression in plants. Annu Rev Plant Physiol Plant Mol Biol 47:509–540

Koch KE, Avigne WT (1990) Postphloem, nonvascular transfer in citrus: kinetics, metabolism, and sugar gradients. Plant Physiol 93:1405–1416

Komatsu A, Moriguchi T, Koyama K, Omura M, Akihama T (2002) Analysis of sucrose synthase genes in citrus suggests different roles and phylogenetic relationships. J Exp Bot 53:61–71

Kruft V, Eubel H, Jansch L, Werhahn W, Braun H-P (2001) Proteomic approach to identify novel mitochondrial proteins in Arabidopsis. Plant Physiol 127:1694–1710

Kuhn C, Hajirezaei M-R, Fernie AR, Roessner-Tunali U, Czechowski T, Hirner B, Frommer WB (2003) The sucrose transporter *stsut1* localizes to sieve elements in potato tuber phloem and influences tuber physiology and development. Plant Physiol 131:102–113

Lalonde S, Wipf D, Frommer WB (2004) Transport mechanisms for organic forms of carbon and nitrogen between source and sink. Annu Rev Plant Biol 55:341–372

Lister R, Chew O, Lee M-N, Heazlewood JL, Clifton R, Parker KL, Millar AH, Whelan J (2004) A transcriptomic and proteomic characterization of the Arabidopsis mitochondrial protein import apparatus and its response to mitochondrial dysfunction. Plant Physiol 134:777–789

Lonosky PM, Zhang X, Honavar VG, Dobbs DL, Fu A, Rodermel SR (2004) A proteomic analysis of maize chloroplast biogenesis. Plant Physiol 134:560–574

Lowell CA, Tomlinson PT, Koch KE (1989) Sucrose-metabolizing enzymes in transport tissues and adjacent sink structures in developing citrus fruit. Plant Physiol 90:1394–1402

Maltman DJ, Simon WJ, Wheeler CH, Dunn MJ, Wait R, Slabas AR (2002) Proteomic analysis of the endoplasmic reticulum from developing and germinating seed of castor (Ricinus communis). Electrophoresis 23:626–639

Millar AH, Sweetlove LJ, Giege P, Leaver CJ (2001) Analysis of the Arabidopsis mitochondrial proteome. Plant Physiol 127:1711–1727

Molendijk AJ, Ruperti B, Palme K (2004) Small GTPases in vesicle trafficking. Curr Opin Plant Biol 7:694–700

Müller ML, Irkens-Kiesecker U, Kramer D, Taiz L (1997) Purification and reconstitution of the vacuolar H+-ATPases from lemon fruits and epicotyls. J Biol Chem 272:12762–12770

Nesvizhskii AI, Keller A, Kolker E, Aebersold R (2003) A statistical model for identifying proteins by tandem mass spectrometry. Anal Chem 75:4646–4658

Oparka KJ, Turgeon R (1999) Sieve elements and companion cells-traffic control centers of the phloem. Plant Cell 11:739–750

Patrick JW (1997) Phloem unloading: sieve element unloading and post-sieve element transport. Annu Rev Plant Physiol Plant Mol Biol 48:191–222

Peltier JB, Friso G, Kalume DE, Roepstorff P, Nilsson F, Adamska I, van Wijk KJ (2000) Proteomics of the chloroplast: systematic identification and targeting analysis of lumenal and peripheral thylakoid proteins. Plant Cell 12:319–341

Perkins DN, Pappin DJC, Creasy DM, Cottrell JS (1999) Probability-based protein identification by searching sequence databases using mass spectrometry data. Electrophoresis 20:3551–3567

Pracharoenwattana I, Cornah JE, Smith SM (2005) Arabidopsis peroxisomal citrate synthase is required for fatty acid respiration and seed germination. Plant Cell 17:2037–2048

Pratelli R, Sutter JU, Blatt MR (2004) A new catch in the SNARE. Trends Plant Sci 9:187–195

Roberts AG, Cruz SS, Roberts IM, Prior D, Turgeon R, Oparka KJ (1997) Phloem unloading in sink leaves of *Nicotiana Benthamiana*: comparison of a fluorescent solute with a fluorescent virus. Plant Cell 9:1381–1396

Ruan Y-L, Patrick JW (1995) The cellular pathway of postphloem sugar transport in developing tomato fruit. Planta V196:434–444

Sadka A, Dahan E, Cohen L, Marsh KB (2000a) Aconitase activity and expression during the development of lemon fruit. Physiol Plant 108:255–262

Sadka A, Dahan E, Or E, Cohen L (2000b) NADP(+)-isocitrate dehydrogenase gene expression and isozyme activity during citrus fruit development. Plant Sci 158:173–181

Sanderfoot AA, Assaad FF, Raikhel NV (2000) The Arabidopsis genome. An abundance of soluble N-ethylmaleimide-sensitive factor adaptor protein receptors. Plant Physiol 124:1558–1569

Shimada T, Nakano R, Shulaev V, Sadka A, Blumwald E (2006) Vacuolar citrate/H+ symporter of citrus juice cells. Planta 224:472–480

Slabas AR, Ndimba B, Simon WJ, Chivasa S (2004) Proteomic analysis of the Arabidopsis cell wall reveals unexpected proteins with new cellular locations. Biochem Soc Trans 32:524–528

Spiegel-Roy P, Goldschmidt EE (1996) Biology of citrus. Cambridge University Press, Cambridge

Surpin M, Raikhel N (2004) Traffic jams affect plant development and signal transduction. Nat Rev Mol Cell Biol 5:100–109

Tanaka N, Fujita M, Handa H, Murayama S, Uemura M, Kawamura Y, Mitsui T, Mikami S, Tozawa Y, Yoshinaga T, Komatsu S (2004) Proteomics of the rice cell: systematic identification of the protein populations in subcellular compartments. Mol Genet Genomics 271:566–576

Tomlinson PT, Duke ER, Nolte KD, Koch KE (1991) Sucrose synthase and invertase in isolated vascular bundles. Plant Physiol 97:1249–1252

Uemura T, Ueda T, Ohniwa RL, Nakano AKT, Sato MH (2004) Systematic analysis of SNARE molecules in Arabidopsis: dissection of the post-golgi network in plant cells. Cell Struct Func 29:49–65

Vandercook CE (1977) Organic acids. In: Nagy S, Shaw PE, Veldhius MK (eds) Citrus fruit technology. Avi Publishing, Westport, CT, pp 209–227

Vernoud V, Horton AC, Yang Z, Nielsen E (2003) Analysis of the small GTPase gene superfamily of Arabidopsis. Plant Physiol 131:1191–1208

Viola R, Roberts AG, Haupt S, Gazzani S, Hancock RD, Marmiroli N, Machray GC, Oparka KJ (2001) Tuberization in potato involves a switch from apoplastic to symplastic phloem unloading. Plant Cell 13:385–398

Wang X, Xu YY, Han Y, Bao SL, Du JZ, Yuan M, Xu ZH, Chong K (2006) Overexpression of RAN1 in rice and Arabidopsis alters primordial meristem, mitotic progress, and sensitivity to auxin. Plant Physiol 140:91–101

Wheeler MCG, Tronconi MA, Drincovich MF, Andreo CS, Flugge U-I, Maurino VG (2005) A comprehensive analysis of the NADP-malic enzyme gene family of Arabidopsis. Plant Physiol 139:39–51

Ytterberg AJ, Peltier J-B, van Wijk KJ (2006) Protein profiling of plastoglobules in chloroplasts and chromoplasts. A surprising site for differential accumulation of metabolic enzymes. Plant Physiol 140:984–997

Zerial M, McBride H (2001) Rab proteins as membrane organizers. Nat Rev Mol Cell Biol 2:107–117

Zhang L-Y, Peng Y-B, Pelleschi-Travier S, Fan Y, Lu Y-F, Lu Y-M, Gao X-P, Shen Y-Y, Delrot S, Zhang D-P (2004) Evidence for apoplasmic phloem unloading in developing apple fruit. Plant Physiol 135:574–586